https://doi.org/10.5194/egusphere-2026-2643
Preprint. Discussion started: 6 July 2026

Long-term evolution and type-specific rainy-season activity of post-seismic geohazards in Southwest China

Hongyu Duan[1],Guoxiang Tu[1,*], Han Liu[1]

[1] State Key Laboratory of Geohazard Prevention and Geoenvironment Protection, Chengdu University of Technology, Chengdu, 610059, China

[*] Corresponding author. Email:: pyk@cdut.edu.cn

https://doi.org/10.5194/egusphere-2026-2643
Preprint. Discussion started: 6 July 2026

Abstract:

Long-term evolution of post-seismic geohazards represents a critical yet complex challenge in earthquake-affected regions. This study systematically investigates the spatiotemporal patterns of post-seismic geohazard evolution following three major seismic events: the 2008 Wenchuan earthquake (Mw7.9), 2013 Lushan earthquake (Mw6.6), and 2017 Jiuzhaigou earthquake (Mw7.0), focusing on four representative counties (Wenchuan, Beichuan, Lushan, and Jiuzhaigou County) in Southwest China. The results show that: (1) post-seismic geohazard activity showed an intermittent clustered outbreak pattern; (2) geohazards were mainly concentrated in valley-related geomorphic units, with county-level differences characterized by reactivation–expansion, spatial inheritance, localization, and contraction; (3) monthly records excluding earthquake-month records showed a clear rainy-season concentration, with 78.1% of geohazards occurring from June to August; and (4) Beichuan and Lushan showed clearer weakening trends, whereas Wenchuan and Jiuzhaigou remained in low-level persistent activity stages and should receive continued monitoring attention. These findings provide useful insights for long-term geohazard monitoring and risk mitigation in earthquake-affected mountainous regions.

Keywords: Post-seismic geohazards; Intermittent clustered outbreak; Spatial evolution; Rainy-season activity; Type-specific response

1. Introduction

Large earthquakes often trigger cascading geological hazards that pose long-term threats to human settlements and critical infrastructure. The 2008 Wenchuan earthquake (Mw 7.9), for example, generated over 56,000 landslides and 200,000 rock falls across an affected area

https://doi.org/10.5194/egusphere-2026-2643
Preprint. Discussion started: 6 July 2026

exceeding 110,000 km² (Huang & Li, 2009; Dai et al., 2011; Gorum et al., 2011; Fan et al., 2018). Similar patterns were observed following the 2013 Lushan (Mw 6.6) and 2017 Jiuzhaigou (Mw 7.0) earthquakes, which induced tens of thousands of secondary geohazards, particularly in mountainous regions (Xu & Xu, 2014; Fan et al., 2019). Globally, seismic events such as the 2010 Maule (Mw 8.8), 2016 Kaikōura (Mw 7.8), and 2009 L'Aquila (Mw 6.3) earthquakes have demonstrated comparable cascading effects, triggering widespread slope instabilities that persist for years (Moro et al., 2016; Massey et al., 2018; Basilone et al., 2019; Serey et al., 2019; Tanyaş et al., 2022).

Beyond immediate coseismic effects, strong ground shaking induces profound geological and ecological disturbances. Seismic waves fracture bedrock, weaken slope structures, and generate deep-seated discontinuities that may later evolve into failure surfaces of rock masses (Huang et al., 2012; He et al., 2020). Post-earthquake assessments in the Wenchuan region revealed extensive rock mass fragmentation, with fracture densities increasing by factors of 2-5 near fault zones (Parker et al., 2011; Zhang et al., 2015; Chen et al., 2020; Chen et al., 2022; Xiong et al., 2022). Comparable degradation was documented after the 1999 Chi-Chi earthquake (Mw 7.6), where persistent slope instability was linked to seismic fracturing (Lin et al., 2003; Hovius et al., 2011; Shou et al., 2011). Additionally, vegetation as a key stabilizing factor is severely disrupted. The Wenchuan earthquake destroyed 3.6×10^5 ha of forest (Liu et al., 2010; Yang et al., 2018; Yunus et al., 2020; Lv et al., 2025).

The resulting rock masses were characterized by high porosity and low mechanical properties, and remained a high potential of rainfall-triggered failures. Prolonged weathering, freeze-thaw cycles, and gravitational stresses progressively weaken these materials and

https://doi.org/10.5194/egusphere-2026-2643
Preprint. Discussion started: 6 July 2026

induced recurrent instabilities (Iverson, 1997; Marc et al., 2015). For instance, landslide activity persisted for over 15 years following the 2005 Kashmir earthquake (Mw 7.6), driven by ongoing weathering of fractured bedrock (Bacha et al., 2022). Moreover, these rock masses serve as primary sources for rainfall-induced debris flows, and extended the hazard durations (Zhu et al., 2011; Zhang & Zhang, 2017; Jin et al., 2023).

Global observations consistently demonstrate that post-seismic geohazards often exhibit protracted activity and could persist from several years to decades. Landslides triggered by the 1906 San Francisco earthquake (Mw 7.9) reactivated for over 50 years in the California Coast Ranges due to rainfall-induced remobilization of seismic debris (Keefer et al., 1987). In some areas, geohazard activities returned to pre-earthquake level within years (Hovius et al., 2011; Minato et al., 2012; Unjoh et al., 2012; Marc et al., 2015; Ishitsuka et al., 2017). While in other regions, such as the Wenchuan region, the activity of post-seismic geohazard persisted for over a decade (Fan et al., 2019). Yunus et al. (2020) and Chen et al. (2020) estimated a return to pre-earthquake landslide activity levels within 18-25 years for the Wenchuan region. Recovery to pre-earthquake geohazard baselines typically requires two key processes: erosional removal of unstable materials and vegetation regeneration to restore slope integrity (Chen et al., 2020; Yunus et al., 2020; Shen et al., 2020).

Rainfall is widely recognized as an important external trigger for post-seismic geohazards, as it can exacerbate the instability of earthquake-fragmented rock masses. Infiltration of rainfall increases pore-water pressure, reduces shear strength, and facilitates slope failures (Shou et al., 2011; Marc et al., 2015; Li et al., 2018; Fan et al., 2019; Chen et al., 2022; Shen et al., 2020). Following the 2015 Gorkha earthquake (Mw 7.8), monsoon rains

https://doi.org/10.5194/egusphere-2026-2643
Preprint. Discussion started: 6 July 2026

triggered over 5,000 landslides in a single season, predominantly in seismically weakened zones (Martha et al., 2017; Tian et al., 2020).

Understanding the spatiotemporal evolution of post-seismic hazards is essential for long-term risk mitigation. This work systematically investigates the long-term evolution of post-seismic geohazards across four earthquake-affected counties in Southwest China: Wenchuan, Beichuan, Lushan, and Jiuzhaigou County. The objectives were to: (1) characterize the intermittent clustered-outbreak pattern of recorded post-seismic geohazards; (2) examine the rainy-season concentration of non-earthquake-month geohazard activity and the type-specific responses of landslides, rock falls, and debris flows; and (3) assess regional differences in long-term post-seismic geohazard persistence and recession. These analyses provide a practical basis for long-term monitoring, rainy-season preparedness, and differentiated risk mitigation in earthquake-affected mountainous regions.

2. Study area and geological setting

The study area (Figure 1), including Lushan, Wenchuan, Beichuan, and Jiuzhaigou counties in northwestern Sichuan Province, China, lies within the seismic zone affected by the 2008 Wenchuan earthquake (Mw 7.9). This region occupies a critical geotectonic position along the transitional boundary between the eastern Tibetan Plateau and the Sichuan Basin. It features complex structural geology that includes the prominent Longmenshan and Minjiang fault systems. Since 2008, the study area has witnessed three significant seismic events: The Wenchuan (Mw 7.9), Lushan (Mw 6.6), and Jiuzhaigou (Mw 7.0) earthquakes.

The Mw 7.9 Wenchuan earthquake on 12 May 2008 resulted from rupture along the Yingxiu-Beichuan Fault, a NE-striking thrust fault with a significant right-lateral strike-slip

https://doi.org/10.5194/egusphere-2026-2643
Preprint. Discussion started: 6 July 2026

component within the Longmenshan Fault Zone. The coseismic rupture propagated over 240 km, producing a maximum vertical displacement of 6.2 m. On 20 April 2013, the Mw 6.6 Lushan earthquake ruptured the southern segment of the Longmenshan Fault Zone, generating a 40 km long surface rupture dominated by thrust faulting mechanisms. Subsequently, the Mw 7.0 Jiuzhaigou earthquake on 8 August 2017 occurred along a left-lateral strike-slip fault within the eastern Kunlun fault system, demonstrating distinct kinematic behavior compared to the preceding events.

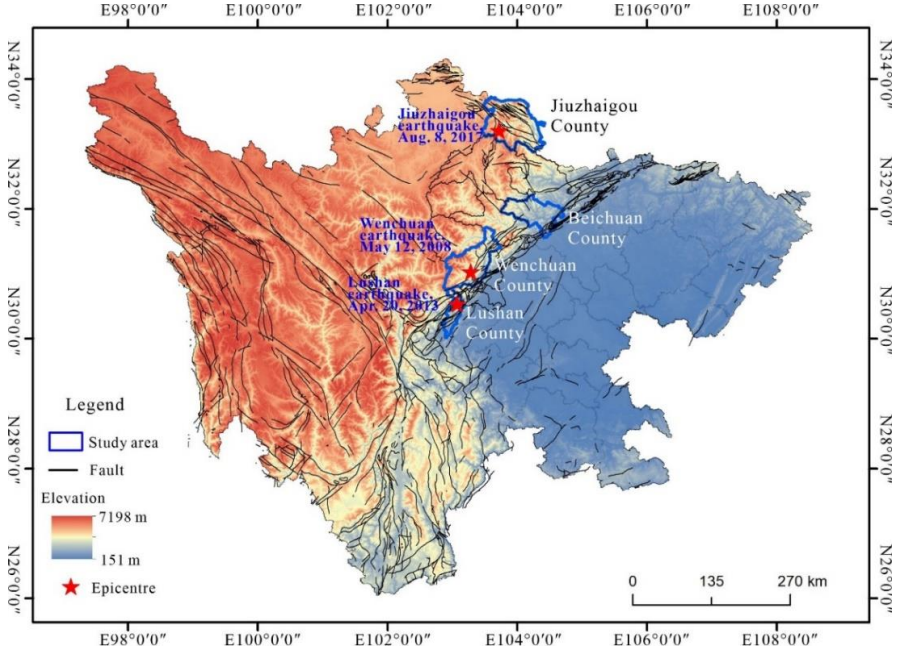

Figure 1 Location of the four earthquake-affected counties in Southwest China.

Major seismic events induced widespread coseismic geohazards across the affected region and caused substantial mountain fracturing and vegetation disturbance. These processes generated unstable rock–soil masses with loose and fragmented structures in the affected slopes (Figure 2). Subsequent rainfall may promote the reactivation or remobilization

https://doi.org/10.5194/egusphere-2026-2643
Preprint. Discussion started: 6 July 2026

of these earthquake-disturbed materials and contribute to the occurrence of post-seismic geohazards (Figure 3). Therefore, the four counties provide a useful setting for examining the long-term evolution of post-seismic geohazards, owing to the documented coseismic impacts and the availability of long-term geohazard and rainfall records.

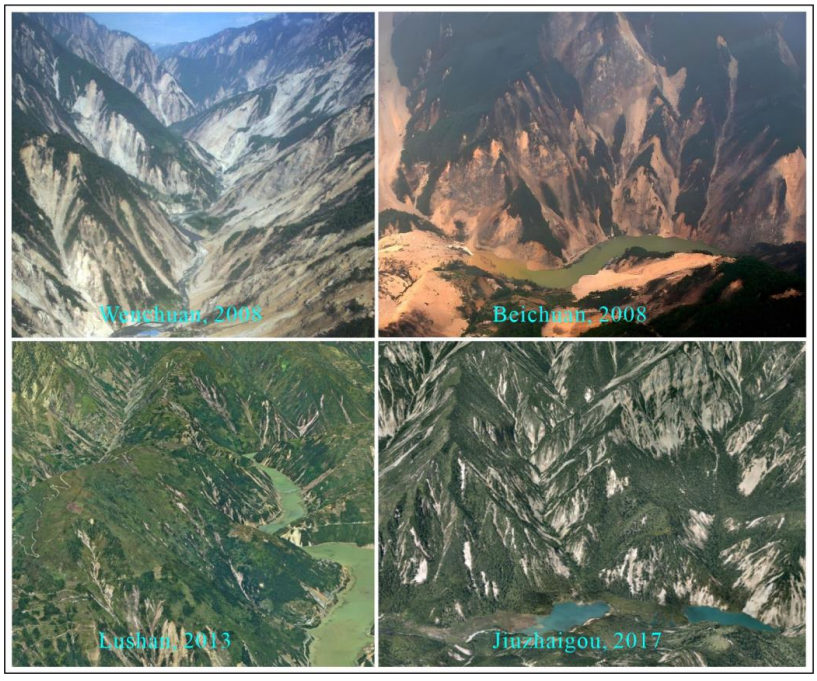

Figure 2 Earthquake-disturbed fractured rock masses and loose slope materials in the study area.

https://doi.org/10.5194/egusphere-2026-2643
Preprint. Discussion started: 6 July 2026

Figure 3 Representative post-seismic geohazards in the study area, including landslides, rock falls, and debris flows.

3. Data and analytical methods

The geohazard inventory used in this study consists of statistical records from the four earthquake-affected counties between 2006 and 2023. These data were mainly derived from the long-term monitoring records of the Sichuan Provincial Geological Environment Monitoring Station and were checked and verified by professional geological survey teams. With continuous temporal coverage, the dataset can serve as a reliable and authoritative source for analyzing post-seismic geohazard activity. In this study, "geohazards" refers to three types of recorded slope-related hazards: landslides, rock falls, and debris flows. Landslides denote sliding failures of soil or rock–soil masses, rock falls denote rapid falling of rock blocks from steep slopes or cliffs, and debris flows denote water–sediment flows

https://doi.org/10.5194/egusphere-2026-2643
Preprint. Discussion started: 6 July 2026

along gullies or channels. These categories were retained from the source database and were not further subdivided because consistent information on failure geometry and movement style was unavailable. It should be noted that the inventory was primarily compiled for geohazard prevention and risk management. Therefore, events threatening settlements, roads, infrastructure, and production areas were preferentially recorded, whereas events in remote uninhabited high-altitude areas were not systematically included. The dataset should therefore be interpreted as a risk-oriented geohazard inventory rather than a complete geomorphic inventory of all mass movements in the study area.

In this work, a total of 4,039 detailed data on geohazards were collected from the four counties, among which 1,281 events were from Wenchuan County (including 537 landslides, 456 rock falls and 288 debris flows), 1,384 events from Beichuan County (including 1085 landslides, 95 rock falls and 204 debris flows), 493 events from Lushan County (including 164 landslides, 263 rock falls and 66 debris flows), and 881 events from Jiuzhaigou County (including 270 landslides, 369 rock falls and 242 debris flows).

To reduce subjective identification, a clustered geohazard outbreak year was operationally defined as a year in which the annual number of recorded geohazards exceeded the county-specific mean annual count during the observation period. The corresponding mean values were 75 for Wenchuan, 77 for Beichuan, 29 for Lushan, and 52 for Jiuzhaigou. This criterion was used to identify relative high-activity years within each county, rather than to define an absolute hazard-frequency threshold. The geohazard distribution maps were generated in ArcGIS using the recorded event locations. The selected representative years correspond to earthquake years, clustered outbreak years, or rainfall-rich years. These maps

https://doi.org/10.5194/egusphere-2026-2643
Preprint. Discussion started: 6 July 2026

show events recorded in the selected year only, rather than cumulative inventories from previous years.

Precipitation data were obtained from a network of 293 rainfall monitoring stations distributed across the study area, including 61 stations in Wenchuan County, 88 in Beichuan County, 54 in Lushan County, and 90 in Jiuzhaigou County. Station rainfall data were used to calculate annual and monthly rainfall series for the four counties. The spatial distribution of these rainfall stations is illustrated in Figure 4. Monthly geohazard records were further grouped into landslides, rock falls, and debris flows to examine the type composition of clustered outbreak months.

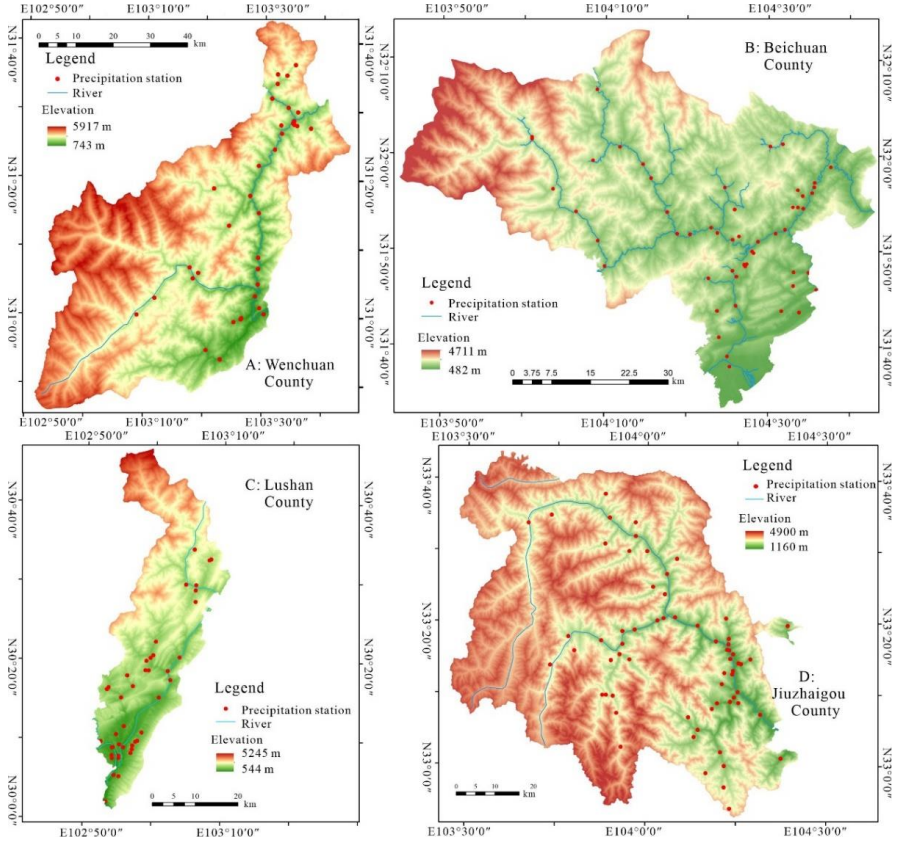

Figure 4 Locations of precipitation stations in the four counties.

https://doi.org/10.5194/egusphere-2026-2643
Preprint. Discussion started: 6 July 2026

4. Results

4.1 Annual evolution of geohazards during the observation period

Figure 5 presents the annual counts of geohazards and the corresponding annual rainfall in the four counties from 2006 to 2023.

In Wenchuan and Beichuan counties, the 2008 Wenchuan earthquake corresponded to clear annual peaks, with 621 and 205 geohazard events, respectively. In Lushan County, only three events were recorded in 2008, indicating a limited response to the Wenchuan earthquake, whereas the 2013 Lushan earthquake corresponded to a sharp increase to 115 events. In Jiuzhaigou County, the annual count increased to 91 events in 2008, indicating an evident response to the Wenchuan earthquake, and reached 358 events in 2017, corresponding to the Jiuzhaigou earthquake.

According to the county-specific mean-count criterion defined in Section 3, the clustered geohazard outbreak years were identified as 2008, 2013, and 2017 for Wenchuan; 2008, 2013, 2018, and 2020 for Beichuan; 2013, 2014, and 2020 for Lushan; and 2008, 2013, 2017, and 2018 for Jiuzhaigou. Between these clustered outbreak years, relatively low-activity periods were observed. For example, Wenchuan decreased to 25–55 events during 2009–2012 and 5–32 events after 2017; Beichuan decreased to 1–7 events during 2009–2012; Lushan fluctuated between 1 and 12 events during 2015–2019; and Jiuzhaigou fluctuated between 15 and 48 events during 2009–2012.

Overall, the four counties experienced two to three clustered geohazard outbreaks after the major earthquakes. These outbreaks were separated by relatively low-activity periods rather than continuous high activity, showing an intermittent outbreak pattern. In addition,

https://doi.org/10.5194/egusphere-2026-2643
Preprint. Discussion started: 6 July 2026

some clustered geohazard outbreak years coincided with years of above-average rainfall, preliminarily suggesting a possible rainfall correspondence. The geohazard type compositions also differed among the four counties: Wenchuan contained comparable numbers of landslides, rock falls, and debris flows; Beichuan was dominated by landslides; and rock falls accounted for a relatively large proportion in Jiuzhaigou and Lushan.

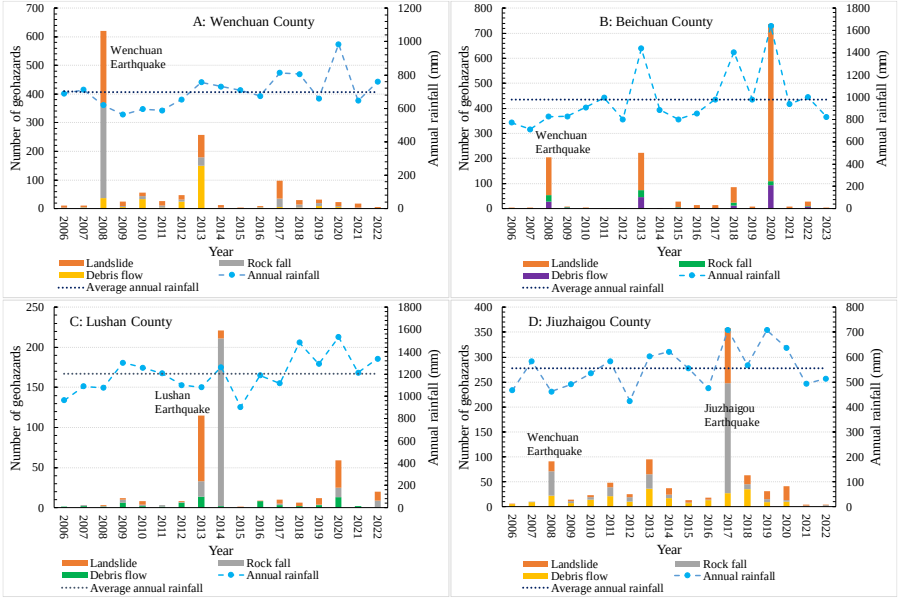

Figure 5 Long-term evolutions of geohazards and annual rainfalls in the four counties from 2006 to 2023.

4.2. Spatial distribution of post-seismic geohazards in representative years

To further clarify the spatiotemporal evolution of post-seismic geohazards, this section focuses on their spatial characteristics in representative years. Based on the annual evolution identified in Section 4.1, earthquake years, clustered outbreak years, and rainfall-rich years were selected to examine where geohazards were concentrated and whether their spatial patterns changed during different stages of post-seismic evolution.

https://doi.org/10.5194/egusphere-2026-2643
Preprint. Discussion started: 6 July 2026

4.2.1 Wenchuan County

The 2008 Wenchuan earthquake induced a large number of coseismic geohazards, mainly rock falls and landslides, which were recorded primarily along major valleys (Figure 6-A). In 2013, geohazards were still mainly recorded along valley slopes and drainage areas, but debris flows became more prominent (Figure 6-B). In 2017 and 2020, the number of events further decreased, while most recorded geohazards remained located in valley-related areas (Figure 6-C). Notably, although annual rainfall was high in 2020, only a small number of geohazards were recorded (Figure 6-D). Overall, Wenchuan showed a relatively stable valley-related distribution pattern in the available records, whereas the activity intensity and dominant geohazard types changed through time.

https://doi.org/10.5194/egusphere-2026-2643
Preprint. Discussion started: 6 July 2026

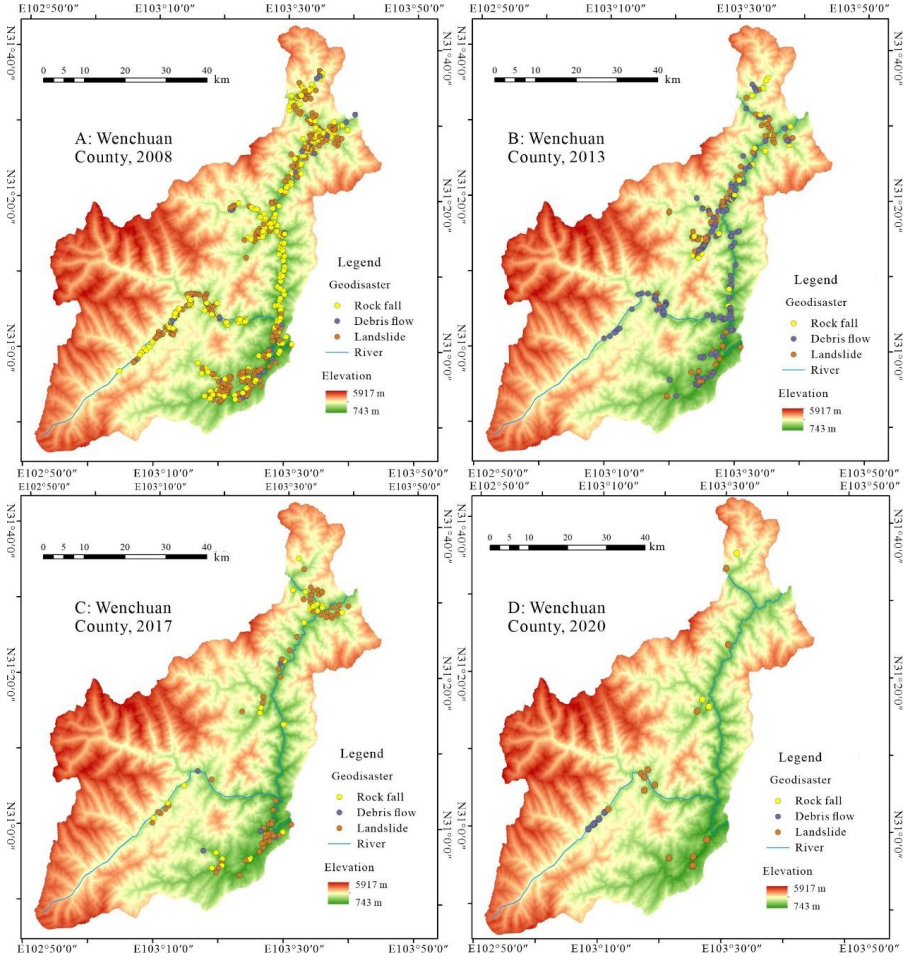

Figure 6 Spatial distribution of recorded geohazards in representative years in Wenchuan County.

4.2.2 Beichuan County

In Beichuan County, the 2008 Wenchuan earthquake triggered a clear coseismic geohazard response, with events mainly distributed along valley flanks (Figure 7-A). In 2013, the number of geohazards exceeded that of the coseismic events in 2008, and the events were distributed over a wider area without a pronounced regional concentration (Figure 7-B). This suggests that post-seismic activity in Beichuan was not confined to the initial coseismic

https://doi.org/10.5194/egusphere-2026-2643
Preprint. Discussion started: 6 July 2026

concentration zones, but involved more widespread reactivation of earthquake-disturbed slopes. In 2018, the number of geohazards decreased, although the distribution remained relatively scattered, with most events located in the northern part of the county (Figure 7-C). In 2020, Beichuan experienced the strongest clustered geohazard outbreak during the observation period. These events were mainly concentrated in the northern and western regions, showing a spatial pattern substantially different from the 2008 coseismic distribution (Figure 7-D). This indicates that later post-seismic activity became more spatially selective and was concentrated in specific subregions where unstable slope materials remained susceptible to failure. Overall, geohazard activity in Beichuan County was dominated by landslides throughout the observation period; its post-seismic evolution was therefore mainly expressed as a change from relatively widespread distribution to localized concentration.

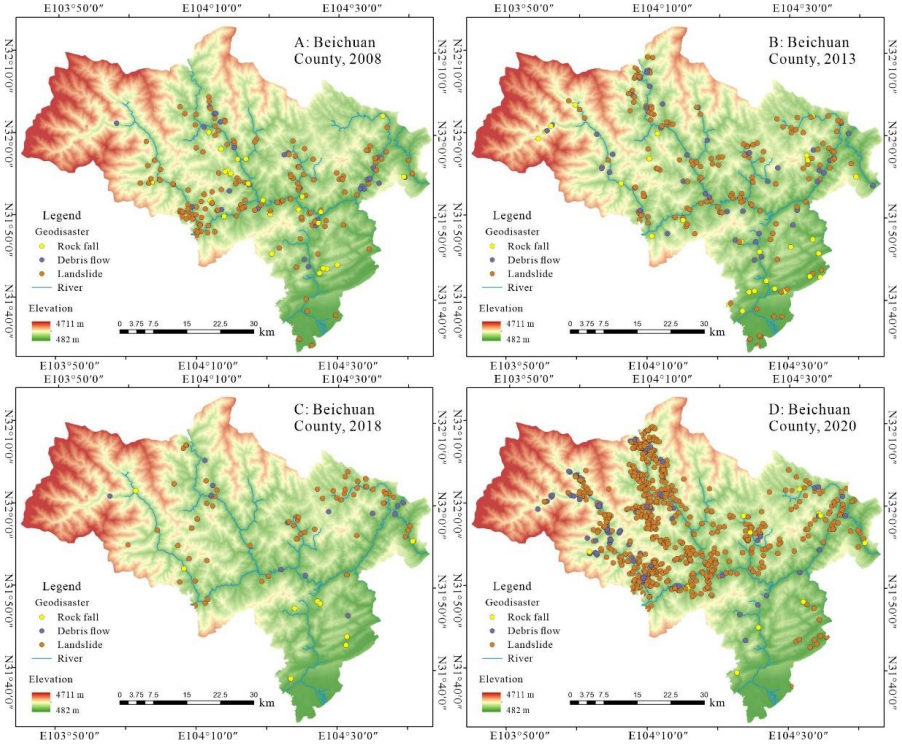

https://doi.org/10.5194/egusphere-2026-2643
Preprint. Discussion started: 6 July 2026

Figure 7 Spatial distribution of recorded geohazards in representative years in Beichuan County.

4.2.3 Lushan County

In Lushan County, the 2013 Lushan earthquake triggered a large number of coseismic geohazards, which were mainly concentrated along valley areas and dominated by landslides (Figure 8-A). In 2014, the total number of geohazards increased to nearly twice that in the coseismic year, with rock falls becoming the dominant type and mainly distributed in the central part of the county (Figure 8-B). In 2018 and 2020, only limited numbers of geohazards were recorded, mainly in the southern region (Figures 8-C and 8-D). The relatively smaller magnitude of the Lushan earthquake, compared with the 2008 Wenchuan earthquake and the 2017 Jiuzhaigou earthquake, may partly explain the delayed post-seismic response in this county, as well as the clear decrease in geohazard counts and spatial contraction over time.

https://doi.org/10.5194/egusphere-2026-2643
Preprint. Discussion started: 6 July 2026

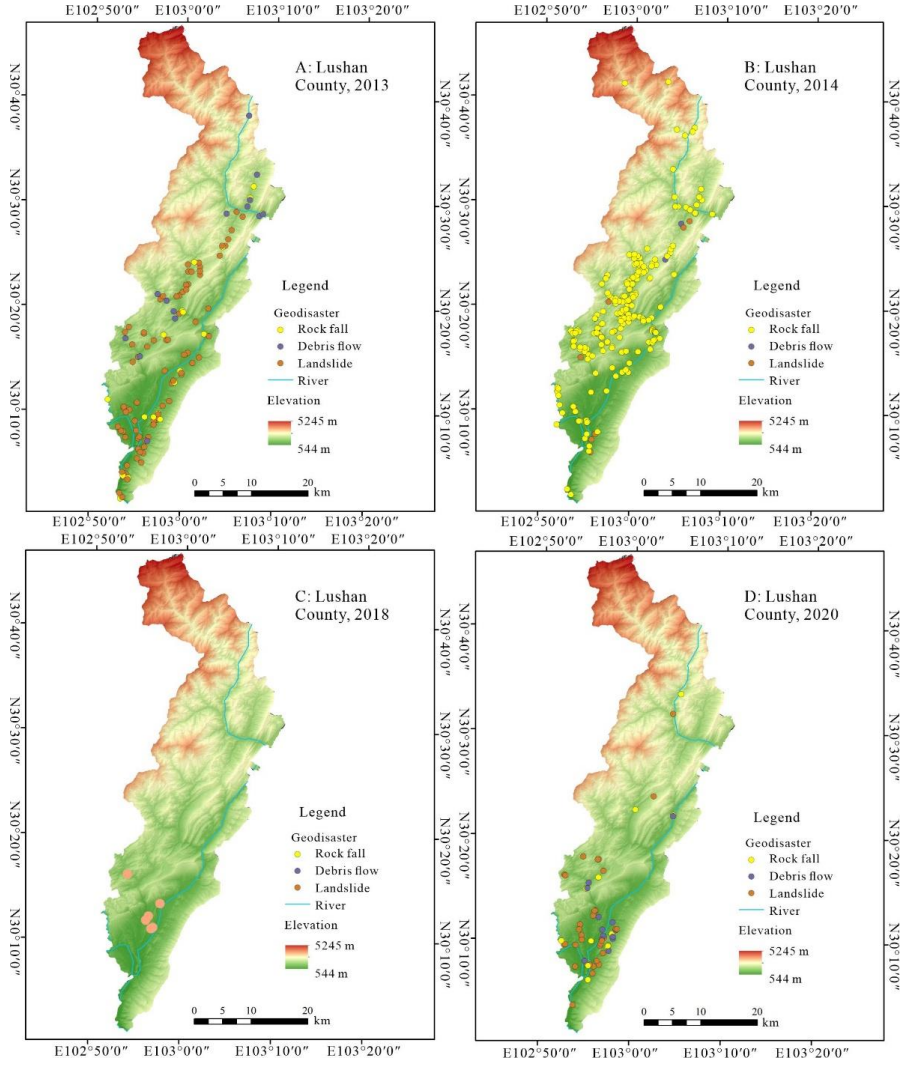

Figure 8 Spatial distribution of recorded geohazards in representative years in Lushan County.

4.2.4 Jiuzhaigou County

In Jiuzhaigou County, the 2008 Wenchuan earthquake was associated with an increase in geohazard activity, with events mainly occurring within mountain valleys and dominated by rock falls (Figure 9-A). In 2013, the first post-seismic clustered outbreak was recorded, and the events were still mainly concentrated in the central and southern valley areas (Figure 9-B).

https://doi.org/10.5194/egusphere-2026-2643
Preprint. Discussion started: 6 July 2026

In 2017, the Jiuzhaigou earthquake triggered a sharp increase in coseismic geohazards, which were dominated by rock falls and mainly distributed in the central and western high-mountain valleys (Figure 9-C). In 2020, the number of geohazards decreased to 41, and the events were mainly concentrated in the southern region (Figure 9-D), indicating that later activity did not completely disappear but became more localized.

The four county cases indicate that post-seismic geohazard evolution showed both common spatial constraints and clear regional differences. A common feature is that recorded geohazards were mainly distributed along valleys, valley slopes, drainage areas, and high-mountain valley settings, reflecting the importance of valley-related geomorphic units in earthquake-affected mountainous regions. However, the spatial evolution differed among counties. These differences show that post-seismic geohazard evolution was expressed not only by changes in annual event counts, but also by spatial persistence, localization, and changes in dominant geohazard types.

https://doi.org/10.5194/egusphere-2026-2643
Preprint. Discussion started: 6 July 2026

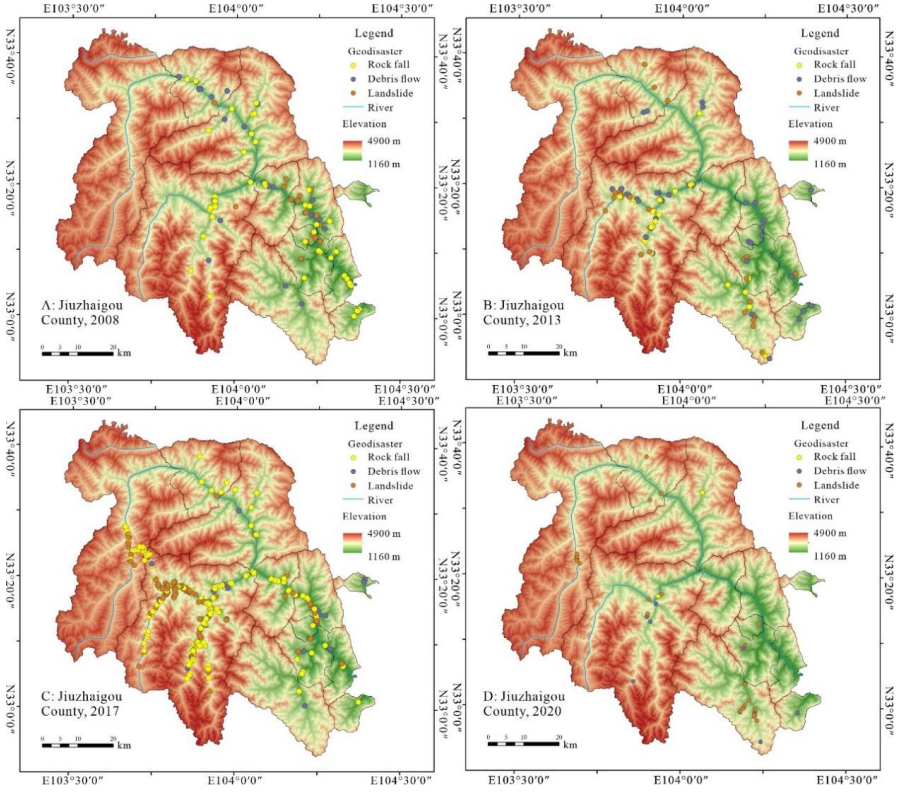

Figure 9 Spatial distribution of recorded geohazards in representative years in Jiuzhaigou County.

4.3 Monthly type-specific geohazard activity and rainfall

Based on the annual series shown in Figure 5, several clustered outbreak years coincided with years of above-average rainfall, whereas this correspondence was not consistent across all counties and years. For example, clustered outbreaks in Wenchuan County in 2013 and 2017 and in Beichuan County in 2013 and 2020 occurred during years with rainfall above the local multi-year mean. In contrast, some rainfall-rich years, such as Wenchuan in 2020 and Lushan in 2018, did not show comparable increases in recorded geohazards. Therefore, monthly rainfall and monthly type-specific geohazard records from 2006 to 2023 were further

https://doi.org/10.5194/egusphere-2026-2643
Preprint. Discussion started: 6 July 2026

analyzed to examine the intra-annual timing, rainfall correspondence, and geohazard type composition of high-activity years in the four counties. The results are shown in Figure 10.

The monthly records captured the direct influence of the three major earthquake months. In May 2008, Wenchuan, Beichuan, and Jiuzhaigou recorded 599, 151, and 72 geohazard events, respectively, indicating the pronounced impact of the Wenchuan earthquake on these counties. Rock falls accounted for the largest proportion in Wenchuan and Jiuzhaigou, whereas landslides were more prevalent in Beichuan. Lushan recorded only one event, suggesting a limited direct response to the Wenchuan earthquake. In April 2013, the Lushan earthquake produced a distinct monthly peak in Lushan County, with landslides representing the main recorded type. In August 2017, the Jiuzhaigou earthquake generated a clear monthly peak in Jiuzhaigou County, where rock falls constituted the dominant type.

After excluding the months of the major earthquakes, most identified clustered outbreak months occurred in June, July, or August, corresponding to the rainy season, and clear differences in geohazard type composition were observed among the four counties. In Wenchuan County, the July 2013 geohazard peak was dominated by debris flows, whereas the dominant type shifted to landslides during the July 2017 peak. In Beichuan County, the clustered outbreaks in July 2013 and August 2020 were both dominated by landslides. Lushan County showed a different pattern: the December 2014 peak was mainly composed of rock falls and occurred outside the main rainy season. This non-rainy-season rock-fall peak may reflect a delayed response of earthquake-damaged rock masses under continued weathering, freeze–thaw action, or gravitational adjustment. The August 2020 peak in Lushan was dominated by landslides. In Jiuzhaigou County, the June 2013 peak showed a slightly higher

https://doi.org/10.5194/egusphere-2026-2643
Preprint. Discussion started: 6 July 2026

contribution from debris flows. These differences indicate that earthquake-month geohazard peaks were commonly dominated by rock falls and landslides, whereas rainy-season peaks were more frequently associated with debris flows or landslides.

Beyond these high-activity months, the overall non-earthquake-month records also showed a clear rainy-season concentration. Using June–August as the main rainy-season window, the three geohazard types showed different seasonal patterns after excluding earthquake-month records. During the observation period, 78.1% of non-earthquake-month geohazards occurred from June to August. Among these rainy-season events, landslides accounted for the largest proportion, at 59.1%, followed by debris flows at 29.0% and rock falls at 11.9%. This indicates that landslides and debris flows were the main geohazard types during the rainy season, whereas rock falls showed a weaker rainy-season association. This type-specific difference suggests that landslides and debris flows were more closely related to rainy-season activity, while rock falls were less seasonally constrained.

In summary, the monthly records show that clustered outbreak years had different intra-annual structures. Earthquake-month peaks were mainly associated with immediate slope failures, with rock falls or landslides as the dominant types. After excluding earthquake-month records, most clustered outbreaks occurred during June–August, and 78.1% of non-earthquake-month geohazards were recorded in this period. These rainy-season events were dominated by landslides and debris flows, indicating a stronger rainy-season association for these two types.

https://doi.org/10.5194/egusphere-2026-2643
Preprint. Discussion started: 6 July 2026

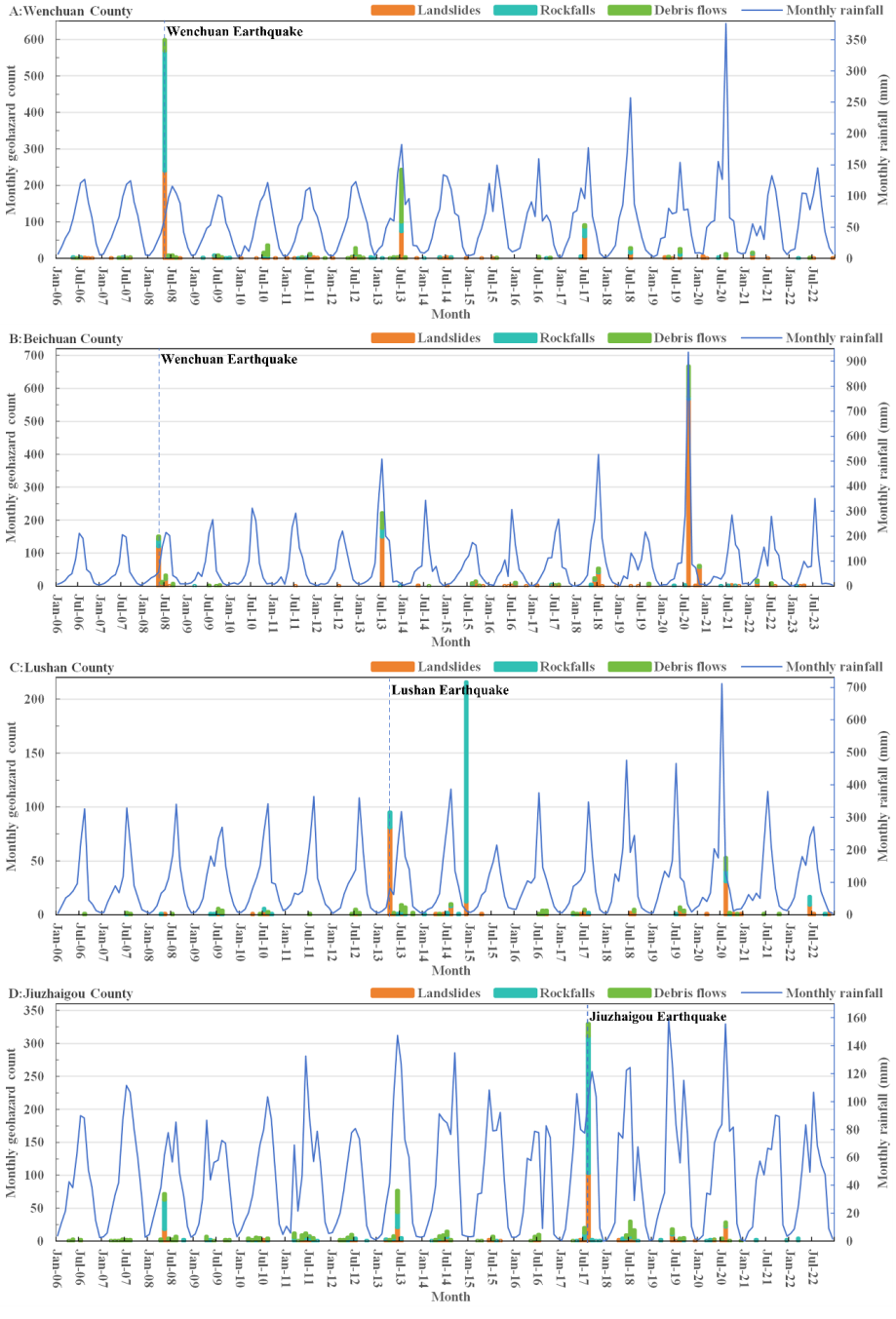

Figure 10 Monthly counts of different geohazard types and monthly rainfall in the four counties from 2006 to 2023

https://doi.org/10.5194/egusphere-2026-2643
Preprint. Discussion started: 6 July 2026

5. Discussion

Since 2006, the study area encompassing four counties has experienced three major seismic events and recurrent post-seismic geohazards. The available event records provide an opportunity to examine how recorded geohazard activity evolved through clustered outbreak years, low-activity intervals, and regional differences in persistence and recession.The fundamental reason for the long-term frequent occurrence of post-earthquake geohazards lies in that abundant rock masses with fragmented structures, poor physical and mechanical properties, and low stability are distributed widely across the affected areas (Iverson, 1997; Marc et al., 2015). Long-term exposure to freeze-thaw cycles, physico-chemical weathering, rainfall, and long-term action of gravitational stress are the major factors for triggering the post-seismic geohazards (Zhu et al., 2011; Zhang & Zhang, 2017; Jin et al., 2023).

Global observational evidence consistently indicates that post-seismic geohazards display protracted activity, often persisting for decades. The notable examples include landslide activity lasting over 15 years in the 2005 Kashmir earthquake (Mw 7.6) region (Bacha et al., 2022), and landslides triggered by the 1906 San Francisco earthquake (Mw 7.9) reactivated for more than 50 years in the California Coast Ranges (Keefer et al., 1987). Similarly, post-seismic geohazard frequencies in the 2008 Wenchuan earthquake area remained 3-5 times higher than pre-seismic levels even 12 years after the earthquake (Fan et al., 2019). In the region affected by the Wenchuan earthquake is supposed to return to pre-earthquake landslide activity levels within 18-25 years (Yunus et al., 2020; Chen et al., 2020). Landslide rates in areas affected by the Chi-Chi earthquake and certain Japanese seismic events have been shown to decay to background levels within 1-6 years (Hovius et al., 2011;

https://doi.org/10.5194/egusphere-2026-2643
Preprint. Discussion started: 6 July 2026

339 Marc et al., 2015).

340 The present study focuses on long-term county-scale event records to identify
341 intermittent clustered outbreak years, spatial differences, regional persistence–recession
342 differences, and monthly type-specific rainy-season activity. Based on our work, the long-
343 term evolution of post-seismic geohazards in the four-county study area exhibits the following
344 characteristics:

345 (1) Annual and monthly records both show that post-seismic geohazard activity did not
346 remain continuously high after the major earthquakes. Instead, it exhibited an intermittent
347 clustered-outbreak pattern, in which high-activity periods were separated by relatively low-
348 activity intervals. The persistent low-level activity during these intervals may reflect a stage
349 of continuous adjustment of earthquake-disturbed slopes and loose materials. After a clustered
350 outbreak, part of the readily mobilized loose material may be transported out of slopes and
351 channels, while the remaining fractured rock–soil masses continue to undergo weathering,
352 freeze–thaw action, rainfall infiltration, and gravitational deformation. In some areas, such as
353 Beichuan, the number of post-seismic clustered geohazard events even exceeded the
354 corresponding coseismic event count. This further indicates that post-seismic geohazard
355 activity did not necessarily weaken continuously after the main earthquake. Instead, its long-
356 term evolution was characterized by alternating high-activity and low-activity periods,
357 reflecting the nonlinear adjustment of earthquake-disturbed slopes.

358 (2) The spatial results reveal both common geomorphic constraints and different spatial
359 evolution modes of post-seismic geohazards. A common feature is that recorded geohazards
360 were mainly distributed along valleys, valley slopes, drainage areas, and high-mountain

https://doi.org/10.5194/egusphere-2026-2643
Preprint. Discussion started: 6 July 2026

valley settings. These valley-related geomorphic units provide steep slopes, free-face conditions, runoff pathways, and loose materials, and they are also the main corridors where settlements, roads, and other exposed elements are distributed. More importantly, the four counties showed different post-seismic spatial evolution modes. Beichuan represents a typical reactivation–expansion mode. After the 2008 coseismic concentration along valley flanks, the 2013 activity became more widely distributed and even exceeded the 2008 coseismic event count, suggesting broader reactivation of earthquake-disturbed slopes. Wenchuan showed clear spatial inheritance of the coseismic geohazard distribution, with later events still mainly concentrated in the valley-related areas where coseismic geohazards had occurred, rather than expanding into new regions. Lushan showed a delayed rock-fall-dominated peak in 2014, followed by a clear decrease in event counts and spatial contraction. Jiuzhaigou experienced a new coseismic peak in 2017, followed by reduced but persistent local activity. These differences indicate that post-seismic spatial evolution may appear as reactivation and expansion, inherited valley-related activity, spatial contraction, or localized persistence in different earthquake-affected regions.

(3) After excluding earthquake-month records, monthly geohazard activity was clearly concentrated in the rainy season from June to August, with 78.1% of events occurring during these three months, indicating a close association between rainfall and post-seismic geohazard activity. Among these rainy-season events, landslides and debris flows were the dominant types, together accounting for 88.1%. More importantly, the dominant geohazard types changed significantly after the earthquakes. Earthquake-month peaks were commonly dominated by rock falls and landslides, reflecting the immediate response of slopes to strong ground shaking.

https://doi.org/10.5194/egusphere-2026-2643
Preprint. Discussion started: 6 July 2026

In contrast, later rainy-season peaks were more frequently characterized by landslides and debris flows. For landslides, rainfall infiltration may increase soil moisture and pore-water pressure, reduce effective stress and shear strength, and promote the failure or reactivation of earthquake-weakened slopes. For debris flows, rainfall-generated runoff may erode and entrain loose materials stored on slopes, in gullies, and in channels, transforming earthquake-disturbed sediments into debris-flow activity (Shou et al., 2011; Marc et al., 2015; Li et al., 2018; Fan et al., 2019; Chen et al., 2022; Shen et al., 2020; Zhu et al., 2011; Zhang & Zhang, 2017; Jin et al., 2023). By contrast, rock falls are more strongly controlled by fractured rock masses, steep slopes, discontinuity-controlled instability, and earthquake-induced rock damage. The December 2014 rock-fall peak in Lushan provides a typical example: it occurred outside the main rainy season and was more likely related to delayed instability of earthquake-damaged rock masses than to a typical rainy-season response. Therefore, rainfall may promote different forms of post-seismic geohazard activity by weakening earthquake-disturbed slopes and remobilizing loose materials during long-term post-seismic evolution.

(4) The four counties indicate two contrasting trajectories: Beichuan and Lushan showed clearer weakening trends after repeated clustered outbreaks, whereas Wenchuan and Jiuzhaigou still remained in a low-level persistent activity stage. In Beichuan, several post-seismic clustered geohazard events occurred after the 2008 Wenchuan earthquake, and their event counts even exceeded the 2008 coseismic records. However, the subsequent decrease in annual event counts and the concentration of later activity in the northern and western parts of the county suggest that post-seismic activity gradually became more localized, possibly reflecting progressive slope stabilization or substantial removal of readily mobilized materials. Lushan

https://doi.org/10.5194/egusphere-2026-2643
Preprint. Discussion started: 6 July 2026

also experienced post-seismic clustered activity after the 2013 earthquake, especially the delayed rock-fall peak in 2014 and the landslide-dominated activity in 2020. The relatively smaller magnitude of the Lushan earthquake, together with the later decrease in event counts and clear spatial contraction, reflects a more evident weakening trend in this county. By contrast, in Wenchuan, the clustered outbreaks in 2013 and 2017 were much smaller than the 2008 coseismic peak, and later events were still mainly concentrated in the valley-related areas initially affected by the 2008 Wenchuan earthquake. This spatial continuity suggests that areas with previous coseismic failures may have a higher probability of recurrent clustered activity, because they combine favorable geomorphic conditions with long-lasting earthquake-disturbed materials. Fan et al. (2018) also reported that loose and fragmented materials remained on slopes in the Wenchuan earthquake-affected region even after a decade of post-earthquake evolution, providing an important material basis for recurrent post-seismic geohazards. In Jiuzhaigou, the time elapsed since the 2017 earthquake is relatively short, and post-seismic activity decreased but still persisted, indicating that this county may still be in a low-activity adjustment stage after the coseismic peak. Therefore, from a monitoring perspective, Wenchuan and Jiuzhaigou should remain key areas for continued observation. Beichuan and Lushan showed clearer recession signals, but localized residual risks should still be considered, especially in areas where previous clustered geohazard activity overlaps with valley-related geomorphic settings.

Several limitations should be noted. The inventory used in this study is risk-oriented and lacks complete geohazard records from high-altitude and uninhabited areas. Because consistent information on hazard boundaries, spatial extent, and volumes was unavailable, this study used

https://doi.org/10.5194/egusphere-2026-2643
Preprint. Discussion started: 6 July 2026

event counts to characterize long-term geohazard activity. In addition, because rainfall was analyzed at annual and monthly scales, the observed relationship represents rainfall–event correspondence rather than rainfall-triggering thresholds. Despite these limitations, the available county-scale records are still useful for identifying long-term temporal patterns, spatial differences, type-specific rainy-season activity, and regional persistence–recession characteristics of recorded post-seismic geohazards.

6. Conclusions

Wenchuan County, Beichuan County, Lushan County, and Jiuzhaigou County have experienced three strong earthquakes since 2006, including the 2008 Wenchuan earthquake (Mw7.9), the 2013 Lushan earthquake (Mw6.6), and the 2017 Jiuzhaigou earthquake (Mw7.0). These earthquakes triggered a large number of coseismic geohazards and generated abundant loose and fragmented rock masses, providing important material sources for clustered outbreaks of post-seismic geohazards. Taking these four counties as examples, this study investigated the long-term evolution characteristics of post-seismic geohazards and reached the following main conclusions.

(1) Post-seismic geohazards mainly showed an intermittent clustered-outbreak pattern. The alternation between high-activity outbreaks and low-activity intervals suggests a non-linear adjustment process of earthquake-disturbed slopes and loose materials.

(2) Spatially, recorded geohazards commonly concentrated in valley-related geomorphic units, while different counties showed distinct evolution characteristics, including reactivation, spatial inheritance, localization, and contraction.

(3) Monthly records excluding earthquake-month records showed a clear rainy-season

https://doi.org/10.5194/egusphere-2026-2643
Preprint. Discussion started: 6 July 2026

concentration, with 78.1% of geohazards occurring from June to August. Landslides and debris flows accounted for 88.1% of these rainy-season events, indicating that the dominant geohazard types shifted toward rainfall-associated landslides and debris flows.

(4) In terms of evolution trends, Beichuan and Lushan showed relatively clear weakening tendencies, whereas Wenchuan and Jiuzhaigou still remained in low-level persistent activity stages and should receive continued monitoring attention.

Acknowledgements

This work was funded by the National Special Fund for scientific and technological basic resources (Grant No. 2022FY100203) and the National Natural Science Foundation of China (Grant No. 42293350, 42293352). We are grateful for the valuable comments from the editor and the anonymous reviewers.

Conflict of interest

The authors declare that they have no conflicts of interest.

Data availability statement

The datasets used and analyzed during the current study are available from the corresponding author on reasonable request.

References

1. Bacha, A., Shafique, M., Werff, H., 2022. Spatio-temporal landslide inventory and susceptibility assessment using Sentinel-2 in the Himalayan mountainous region of Pakistan. Environ Monit Assess, 194:845, https://doi.org/10.1007/s10661-022-10514-w

https://doi.org/10.5194/egusphere-2026-2643
Preprint. Discussion started: 6 July 2026

2. Basilone, L., Bonfardeci, A., Romano, P., Sulli, A., 2019. Natural Laboratories for Field Observation About Genesis and Landscape Effects of Palaeo-Earthquakes: a Proposal for the Rocca Busambra and Monte Barracu Geosites (West Sicily). Geoheritage, 11:821-837, DOI: 10.1007/s12371-018-0334-8

3. Chen, M., Tang, C., Li, M., et al., 2022. Changes of surface recovery at coseismic landslides and their driving factors in the Wenchuan earthquake-affected area. Catena, 210:105871, https://doi.org/10.1016/j.catena.2021.105871

4. Chen, M., Tang, C., Xiong, J., et al., 2020. The long-term evolution of landslide activity near the epicentral area of the 2008 Wenchuan earthquake in China. Geomorphology, 367:107317, https://doi.org/10.1016/j.geomorph.2020.107317

5. Dai, F.C., Xu, C., Yao, X., Xu, L., Tu, X.B., Gong, Q.M., 2011. Spatial distribution of landslides triggered by the 2008 Ms 8.0 Wenchuan earthquake, China. Journal of Asian Earth Sciences, 40:883-895, DOI: 10.1016/j.jseaes.2010.04.010

6. Fan, X.M., Juang, C., Wasowski, J., et al., 2018. What we have learned from the 2008 Wenchuan Earthquake and its aftermath: A decade of research and challenges. Engineering Geology, 241:25-32, https://doi.org/10.1016/j.enggeo.2018.05.004

7. Fan, X.M., Scaringi, G., Korup, O., et al., 2019. Earthquake-Induced Chains of Geologic Hazards: Patterns, Mechanisms, and Impacts. *Reviews of Geophysics*, 57:421-503, https://doi.org/10.1029/2018RG000626

8. Gorum, T., Fan, X., Westen, C., et al., 2011. Distribution pattern of earthquake-induced landslides triggered by the 12 May 2008 Wenchuan earthquake. Geomorphology, 133:152-167, DOI: 10.1016/j.geomorph.2010.12.030

https://doi.org/10.5194/egusphere-2026-2643
Preprint. Discussion started: 6 July 2026

9. He, J., Qi, S., Wang, Y., et al., 2020. Seismic response of the Lengzhuguan slope caused by topographic and geological effects. Engineering Geology, 265, DOI: 10.1016/j.enggeo.2019.105431
10. Huang, R., Li, W., 2009. Development and distribution of geohazards triggered by the 5.12 Wenchuan Earthquake in China. Science in China Series E: Technological Sciences, 52:810-819, DOI: 10.1007/s11431-009-0117-1
11. Huang, R., Pei, X., Fan, X., et al., 2012. The characteristics and failure mechanism of the largest landslide triggered by the Wenchuan earthquake, May 12, 2008, China. Landslides, 9:131-142, DOI: 10.1007/s10346-011-0276-6
12. Hovius, N., Meunier, P., Lin, C., et al., 2011. Prolonged seismically induced erosion and the mass balance of a large earthquake. Earth and Planetary Science Letters, 304:347-355, DOI: 10.1016/j.epsl.2011.02.005
13. Ishitsuka, K., Matsuoka, T., Nishimura, T., et al., 2017. Ground uplift related to permeability enhancement following the 2011 Tohoku earthquake in the Kanto Plain, Japan. Earth, Planets and Space, 69:81, DOI: 10.1186/s40623-017-0666-7
14. Iverson, RM., 1997. The physics of debris flows. *Reviews of Geophysics*, 35:245-296, DOI: 10.1029/97RG00426
15. Jin, W., Cui, P., Zhang, G., 2023. Evaluating the post-earthquake landslides sediment supply capacity for debris flows. Catena, 220:106649, https://doi.org/10.1016/j.catena.2022.106649
16. Keefer, D., Wilson, R., Mark, R., et al., 1987. Real-Time Landslide Warning During Heavy Rainfall. Science, 238:921-925, DOI: 10.1126/science.238.4829.921

https://doi.org/10.5194/egusphere-2026-2643
Preprint. Discussion started: 6 July 2026

17. Li, C., Wang, M., Liu, K., 2018. A decadal evolution of landslides and debris flows after the Wenchuan earthquake. Geomorphology, 323:1-12, https://doi.org/10.1016/j.geomorph.2018.09.010

18. Lin, C., Shieh, C., Yuan, B., et al., 2003. Impact of Chi-Chi earthquake on the occurrence of landslides and debris flows: example from the Chenyulan River watershed, Nantou, Taiwan. Engineering Geology, 71:49-61, DOI: 10.1016/S0013-7952(03)00125-X

19. Liu, Y., Liu, R. & Ge, Q., 2010. Evaluating the vegetation destruction and recovery of Wenchuan earthquake using MODIS data. Nat Hazards, 54:851–862, https://doi.org/10.1007/s11069-010-9511-z

20. Lv, J., He,, X., Bao, Y. et al., 2025. Spatiotemporal pattern of post-earthquake vegetation recovery in a mountainous catchment in southwestern China. Nat Hazards, 121:3023-3046, https://doi.org/10.1007/s11069-024-06918-1

21. Marc, O., Hoviuse, N., Meunier, P., et al., 2015. Transient changes of landslide rates after earthquakes. *Geology*, 43:883-886, DOI: 10.1130/G36961.1

22. Martha, T., Roy, P., Mazumdar, R., et al., 2017. Spatial characteristics of landslides triggered by the 2015 Mw 7.8 (Gorkha) and Mw 7.3 (Dolakha) earthquakes in Nepal. Landslides, 14:697-704, DOI: 10.1007/s10346-016-0763-x

23. Massey, C., Townsend, D., Rathje, E., et al., 2018. Landslides Triggered by the 14 November 2016 Mw 7.8 Kaikōura Earthquake, New Zealand. Bulletin of the Seismological Society of America, 108:1630-1648, DOI: 10.1785/0120170305

https://doi.org/10.5194/egusphere-2026-2643
Preprint. Discussion started: 6 July 2026

24. Minato, S., Tsuji T., Ohmi S., and Matsuoka T., 2012. Monitoring seismic velocity change caused by the 2011 Tohoku-oki earthquake using ambient noise records. Geophys. Res. Lett., 39:L09309, DOI: 10.1029/2012GL051405.

25. Moro, M., Chini M., Saroli, M., et al., 2011. Analysis of large, seismically induced, gravitational deformations imaged by high-resolution COSMO-SkyMed synthetic aperture radar. Geology, 39:527-530, DOI: 10.1130/G31748.1

26. Parker, R., Densmore, A., Rosser, N., et al., 2011. Mass wasting triggered by the 2008 Wenchuan earthquake is greater than orogenic growth. Nature Geoscience, 4:449-452, DOI: 10.1038/NGEO1154

27. Serey, A., Piñero-Feliciangeli, L., Sepúlveda, S.A., et al., 2019. Landslides induced by the 2010 Chile megathrust earthquake: a comprehensive inventory and correlations with geological and seismic factors. Landslides, 16:1153-1165, DOI: 10.1007/s10346-019-01150-6

28. Shen,P., Zhang,L, Fan, Zhu, R., Zhang, S., 2020. Declining geohazard activity with vegetation recovery during first ten years after the 2008 Wenchuan earthquake. Geomorphology, 352:106989, https://doi.org/10.1016/j.geomorph.2019.106989

29. Shou, K., Hong, C., Wu, C., et al., 2011. Spatial and temporal analysis of landslides in Central Taiwan after 1999 Chi-Chi earthquake. Engineering Geology, 123:122-128, DOI: 10.1016/j.enggeo.2011.03.014

30. Tanyaş, H., Görüm, T., Fadel, I., et al., 2022. An open dataset for landslides triggered by the 2016 Mw 7.8 Kaikōura earthquake, New Zealand. Landslides, 19:1405-1420, DOI: 10.1007/s10346-022-01869-9

https://doi.org/10.5194/egusphere-2026-2643
Preprint. Discussion started: 6 July 2026

31. Tian, Y., Owen, L., Xu, C., et al., 2020. Landslide development within 3 years after the 2015 Mw 7.8 Gorkha earthquake, Nepal. Landslides, 17:1251-1267, DOI: 10.1007/s10346-020-01366-x

32. Unjoh, S., Kaneko, M., Kataoka, S., et al., 2012. Effect of earthquake ground motions on soil liquefaction. Soils and Foundations, 52:830-841, DOI: 10.1016/j.sandf.2012.11.006

33. Xiong, J., Tang, C., Tang, H., et al., 2022. Long-term hillslope erosion and landslide–channel coupling in the area of the catastrophic Wenchuan earthquake. Engineering Geology, 305:106727, https://doi.org/10.1016/j.enggeo.2022.106727

34. Xu, C., and Xu, X., 2014. The spatial distribution pattern of landslides triggered by the 20 April 2013 Lushan earthquake of China and its implication to identification of the seismogenic fault. Chinese Science Bulletin, 59:1416-1424, DOI: 10.1007/s11434-014-0202-0

35. Yang, W., Qi, W., Zhou, J., 2018. Decreased post-seismic landslides linked to vegetation recovery after the 2008 Wenchuan earthquake. Ecological Indicators, 89:438-444, https://doi.org/10.1016/j.ecolind.2017.12.006

36. Yunus, A., Fan, X., Tang, X., et al., 2020. Decadal vegetation succession from MODIS reveals the spatio-temporal evolution of post-seismic landsliding after the 2008 Wenchuan earthquake. Remote Sensing of Environment, 236:111476, https://doi.org/10.1016/j.rse.2019.111476

37. Zhang, S., Zhang, L., 2017. Impact of the 2008 Wenchuan earthquake in China on subsequent long-term debris flow activities in the epicentral area. Geomorphology, 276:86-103, http://dx.doi.org/10.1016/j.geomorph.2016.10.009

https://doi.org/10.5194/egusphere-2026-2643
Preprint. Discussion started: 6 July 2026

577 38. Zhang, S., Zhang, L., Lacasse, S., Nadim, F., 2015. Evolution of Mass Movements near
578 Epicentre of Wenchuan Earthquake, the First Eight Years. Scientific RepoRts, 6:36154,
579 DOI: 10.1038/srep36154
580 39. Zhu, J., Ding, J., Liang, J., 2011. Influences of the Wenchuan Earthquake on Sediment
581 Supply of Debris Flows. J. Mt. Sci., 8: 270– 277, DOI: 10.1007/s11629-011-2114-7

582